AD-786 668

TRANSFORMATION CHARACTERISTICS OF QUATERNARY URANIUM-BASE ALLOYS

D. E. Blake, et al

Case Western Reserve University

Prepared for:

Army Materials and Mechanics Research Center
Army Materiel Command

July 1974

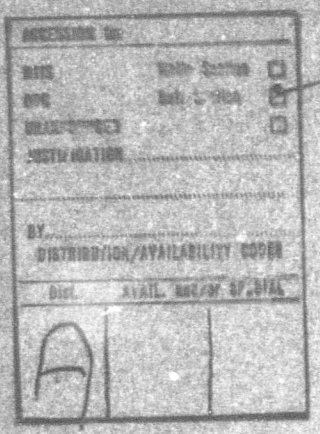

The findings in this report are not to be construed as an official Department of the Army position, unless so designated by other authorized documents.

Mention of any trade names or manufacturers in this report shall not be construed as advertising nor as an official indorsement or approval of such products or companies by the United States Government.

ib

DISPOSITION INSTRUCTIONS

Destroy this report when it is no longer needed.
Do not return it to the originator.

TRANSFORMATION CHARACTERISTICS OF QUATERNARY URANIUM-BASE ALLOYS

Final Report

Conducted for

ARMY MATERIALS AND MECHANICS RESEARCH CENTER
Watertown, Massachusetts

Contract No. DAAG 46●73-C-0130

Technical Monitor: J. Greenspan
D. Colling

D. E. Blake
Graduate Assistant

R. F. Hehemann
Professor

Division of Metallurgy and Materials Science
CASE WESTERN RESERVE UNIVERSITY
Cleveland, Ohio

July, 1974

ic

UNCLASSIFIED

SECURITY CLASSIFICATION OF THIS PAGE (When Data Entered)

AD 786 668

REPORT DOCUMENTATION PAGE

READ INSTRUCTIONS BEFORE COMPLETING FORM

1. REPORT NUMBER: AMMRC CTR 74-51	2. GOVT ACCESSION NO.
3. RECIPIENT'S CATALOG NUMBER	
4. TITLE (and Subtitle): TRANSFORMATION CHARACTERISTICS OF QUATERNARY URANIUM-BASE ALLOYS	5. TYPE OF REPORT & PERIOD COVERED: Final Report
	6. PERFORMING ORG. REPORT NUMBER
7. AUTHOR(s): D. E. Blake and R. F. Hehemann	8. CONTRACT OR GRANT NUMBER(s): DAAG 46073-C-0130
9. PERFORMING ORGANIZATION NAME AND ADDRESS: Army Materials and Mechanics Research Center, Watertown, Massachusetts 02172, AMXMR-	10. PROGRAM ELEMENT, PROJECT, TASK AREA & WORK UNIT NUMBERS: D/A Project: W564603D66300; AMCMS Code: 554C.12.26300; Agency Accession:
11. CONTROLLING OFFICE NAME AND ADDRESS: U. S. Army Materiel Command, Alexandria, Virginia 22304	12. REPORT DATE: July 1974
	13. NUMBER OF PAGES: ~~69~~ 67
14. MONITORING AGENCY NAME & ADDRESS(if different from Controlling Office)	15. SECURITY CLASS. (of this report): Unclassified
	15a. DECLASSIFICATION/DOWNGRADING SCHEDULE

16. DISTRIBUTION STATEMENT (of this Report)

Approved for public release; distribution unlimited.

17. DISTRIBUTION STATEMENT (of the abstract entered in Block 20, if different from Report)

Details of illustrations in this document may be better studied on microfiche.

18. SUPPLEMENTARY NOTES

19. KEY WORDS (Continue on reverse side if necessary and identify by block number)

Titanium alloys
Phase transformations
Time dependence
Hardness

20. ABSTRACT (Continue on reverse side if necessary and identify by block number)

(SEE REVERSE SIDE)

67

DD FORM 1 JAN 73 1473 EDITION OF 1 NOV 65 IS OBSOLETE

UNCLASSIFIED

SECURITY CLASSIFICATION OF THIS PAGE (When Data Entered)

The transformation characteristics of quaternary uranium-base alloys containing small, equal amounts (K) of molybdenum, niobium, and zirconium with 0.5 weight percent titanium were examined by dilatometric, hardness, metallographic and x-ray diffraction techniques. Principal emphasis was placed on isothermal transformacion of an alloy with K = 1.5%. Quench-ageing treatments of this alloy as well as isothermal transformation of an alloy with K = 0.75% were studied less extensively.

When quenched from the γ phase, these alloys transform martensitically to distorted forms of alpha uranium. The isothermal decomposition of the γ phase takes place at distinctly different rates at temperatures above and below M_s. Substantial hardening accompanies the decomposition process in both temperature ranges with a maximum hardness of approximately 55RC developing in the 1.5% quaternary alloy.

The hardening results from precipitation within the matrix of transition and intermediate phases characteristic of U-Ti, -Zr and -Mo systems. Subsequently nucleation and growth of an incoherent form of α uranium occurs which constitutes an overageing reaction and induces substantial softening.

Precipitation of the transition phases from both the BCC uranium and distorted α uranium phases is considered in terms of the stability of these structures to displacement waves.

TRANSFORMATION CHARACTERISTICS OF QUATERNARY URANIUM-BASE ALLOYS

ABSTRACT

The transformation characteristics of quaternary uranium-base alloys containing small, equal amounts (K) of molybdenum, niobium, and zirconium with 0.5 weight percent titanium were examined by dilatometric, hardness, metallographic and x-ray diffraction techniques. Principal emphasis was placed on isothermal transformation of an alloy with K = 1.5%. Quench-ageing treatments of this alloy as well as isothermal transformation of an alloy with K = 0.75% were studied less extensively.

When quenched from the γ phase, these alloys transform martensitically to distorted forms of alpha uranium. The isothermal decomposition of the γ phase takes place at distinctly different rates at temperatures above and below M_S. Substantial hardening accompanies the decomposition process in both temperature ranges with a maximum hardness of approximately 55RC developing in the 1.5% quaternary alloy.

The hardening results from precipitation within the matrix of transition and intermediate phases characteristic of U-Ti, -Zr and -Mo systems. Subsequently, nucleation and growth of an incoherent form of α uranium

occurs which constitutes an overageing reaction and induces substantial softening.

Precipitation of the transition phases from both the BCC uranium and distorted α uranium phases is considered in terms of the stability of these structures to displacement waves.

INTRODUCTION

Many nuclear and non-nuclear applications of depleted uranium, including radiation shielding, armor piercing projectiles and compact gyroscopes (1), are based on its high density. However, the low strength and ductility of pure uranium severely limits its utility. The mechanical properties can be improved significantly with only small penalties on density by alloying combined with appropriate thermal treatments (2). Thus, the mechanical properties of a variety of uranium base alloys have been determined and tensile strengths in the range of 250,000 psi with some retained ductility have been achieved (3-5).

The transformation mechanisms and characteristics of uranium base alloys have been studied rather extensively in order to provide a basis for property control through heat treatment. Frequently, the uranium-molybdenum and uranium-niobium systems have served as models (6-13) for the variety of transformations that occur in these systems.

The transformation characteristics of uranium-base alloys are relatively complex with a variety of metastable states intruding in the transformation sequence. This is particularly evident in structures produced by quenching from the γ field. Specifically, the BCC γ phase transforms

successively through a sequence of metastable states involving

$$\gamma \rightarrow \gamma_d^o \rightarrow \alpha'' \rightarrow \alpha'.$$

The nomenclature of Lehmann and Hills (14) is normally used to designate these phases and, in general, will be employed here. In this system, modifications of the low temperature α-phase are denoted as α with subscripts a, b or n where a and b designate acicular or banded martensitic products and n specifies one formed by nucleation and growth. The structures are further characterized by superscripts in which α' represents a distortion of the orthorhombic structure involving primarily a contraction of the b_o parameter and α'' denotes a monoclinic distortion of the α-phase. γ_d^o also frequently exhibits a banded structure and represents a tetragonal distortion of the BCC phase. Other metastable states also occur in specific systems, and, in particular, a variant of the omega phase occurs in U-Ti and U-Zr alloys (15-17).

In the course of development of uranium-base alloys in recent years, considerable interest has arisen in complex alloys containing several solutes. Quaternary alloys containing equal amounts (K) of molybdenum, niobium and zirconium with 0.5%* titanium, balance uranium, have been the subject of mechanical property investigations.

*Percents are given as weight percent

The mechanical properties of these alloys with K ranging from 0.75% to 2.0% have been documented by the Army Materials and Mechanics Research Center [4] and are summarized by Colling and Greenspan[18]. They have shown that optimum properties in both the as-quenched, and the quenched and aged states are achieved with K equal to 1.5%. While the mechanical properties of these alloys are well known, only limited studies of their transformation mechanisms and characteristics have been performed [4, 18, 19].

This study was undertaken to explore the kinetics and mechanisms of isothermal and quench-age modes of transformation in these quaternary alloys. Primary emphasis was placed on the 905 alloy (K = 1.5%) and some preliminary work on the 904 alloy (K = 0.75%) is also reported.

MATERIALS AND PROCEDURES

The uranium alloys used in this investigation were received from the Army Materials and Mechanics Research Center, Watertown, Massachusetts in the form of 3/4-inch diameter extruded rounds approximately two feet in length. The chemical compositions of the alloys are given in Table I.

Prior to machining, the bars were cut into four-inch lengths to facilitate handling, encapsulated in evacuated fused quartz tubes, homogenized at 1750°F (960°C) for five hours, and water quenched. Specimens for metallographic, hardness, dilatometric and x-ray studies were machined from the homogenized bar.

Dilatometry

The dilatometric specimens were 1/16-inch thick, 1/4-inch wide, and 1-1/4-inches long with two 0.125-inch holes drilled on 1-inch centers. The samples were finished on 240 grit silicon carbide paper, etched in concentrated nitric acid and immediately copper plated. Plating was conducted in an acid copper bath at 90-120°F. Plating times of 30 minutes at a current of 0.3 amp resulted in a copper thickness of approximately 0.001 inch.

The dilatometer used consisted of two concentric fused quartz rods. The inner rod activated a linear variable

differential transformer and the amplified signal was recorded on a Moseley strip chart recorder. To monitor the temperature of the specimen, a thermocouple was spot-welded to its center.

The specimen was solutionized in the dilatometer at 1650°F (900°C) for at least 20 minutes in a tube furnace containing a dry argon atmosphere. To obtain the M_s temperature, the sample was air cooled from 1650°F and a dilation versus temperature curve was obtained using an X-Y recorder.

The dilation versus temperature curves used in determining critical temperatures during heating were obtained from samples heated slowly with the furnace, monitoring both dilation and temperature. Preliminary experiments demonstrated that the "as-homogenized" samples experienced ageing reactions during the slow heating which made determination of the critical temperatures difficult. Consequently, the dilatometer samples were aged for five hours at 900°F (482°C) before determining the critical temperatures. The critical temperature phenomena thus were determined only for fully aged structure.

Heat Treating

Copperplated samples were employed for heat-treating times of 250 seconds or less. However, for times longer than 250 seconds, the samples were sealed in fused quartz

capsules which were evacuated to 10^{-4} mm Hg and then filled with 1/4 to 1/2 atmosphere of helium to insure that the transformation temperature was reached as quickly as possible.

The samples were solutionized at 1650°F for twenty minutes in a tube furnace with an atmosphere of dry argon used in the case of the plated samples. At the end of this time, the isothermal samples were transferred to conventional salt pots at the desired transformation temperature. Temperatures were controlled to ±5°F (±3°C). Before transforming at the desired temperature, the ageing samples were quenched into room temperature water from the solutionizing temperature. When the desired transformation or ageing time for both type samples was reached, they were quenched into water at room temperature, breaking the quartz capsules under the water.

Hardness Testing

After heat treating, the hardness samples (1/8 x 1/8 x 3/8 inch) were smoothed on 240 grit paper. A conventional Wilson Rockwell hardness testing machine was used to obtain the R_C hardness. Four readings were taken on each sample and the average of these reported. If the four varied more than two hardness numbers, the previous hardness marks were ground off and the test repeated until consistency was achieved. Microhardness was measured on a Leitz microhardness machine

using a diamond pyramid indenter with a 50 kilogram load.

Metallography

For metallographic examination, the hardness samples were mounted in a cold setting resin. Samples were ground on silicon carbide papers with a water lubricant, and rough polishing was accomplished with a nine micron diamond paste and Buehler Metadi fluid as the lubricant. A 0.05 micron alumina slurry with a 1% HF solution as the lubricant was employed for the final polish.

To remove the distorted surface layer resulting from the mechanical polishing, the samples were electropolished in a solution of one part (118 g CrO_3 : 100 ml H_2O) to four parts glacial acetic acid. The solution was held at 32-35°F (0-3°C) by the use of an ice water bath. The samples were polished at 50 VDC for 30 seconds in increments of five seconds.

The samples were then etched chemically in a solution consisting of:

100 ml	H_2O
5 ml	Conc. HNO_3
10 ml	30% H_2O_2
5 g	DET*

The etchant was stirred and used at room temperature. Etching times ranged from 2 to 40 minutes depending on

*DET - Disodium ethylenediamine tetracetate.

the amount and type of transformation product present. The samples were examined under a Zeiss Ultraphot microscope equipped with Nomarski objectives.

X-ray Diffraction

X-ray diffraction patterns were obtained with a Debye-Scherrer powder camera or a General Electric Company diffractometer using nickel filtered copper radiation. The samples used in the diffractometer were 3/4-inch diameter slugs 1/4-inch thick, and were polished in the same manner as the metallographic samples. The samples used in the powder camera were 1/16 x 1/16 x 1/2 inch thinned to a point on one end. This was accomplished in the electropolishing solution at 20 VDC for 20 to 30 minutes.

RESULTS AND DISCUSSION

Critical Temperatures and the Quenched State of the 905 Alloy.

Dilatometric measurements were used to determine the critical temperatures and the M_s temperature. The dilation curve obtained by slow heating of the fully aged 905 alloy (K = 1.5%) is presented in Fig. 1. The eutectoid temperature A_1 is approximately 1130°F (610°C) and the upper critical A_3 is 1200°F (650°C). In order to determine the M_s temperature, homogenized samples were air cooled (approximately 150°C/min) from 900°C in the dilatometer. As shown on Fig. 2, the M_s temperature was 760°F (404°C). Howlett (8) has shown that the M_s temperatures of U-Mo alloys are relatively insensitive to cooling rate at alloy contents below 10 at % Mo. However, it should be noted that the binary U-Mo alloys transform successively during cooling from γ to γ_d^o to α_b''. There are no indications in Fig. 2 for this successive transformation sequence in this quaternary alloy.

Fig. 3 demonstrates that the martensite formed by water quenching from 900°C exhibits the banded structure typical of the martensites in most of the more highly alloyed uranium alloys. X-ray diffraction data presented in Table 2 indicate that this alloy exhibits the monoclinic α_b'' structure as reported by Colling and Greenspan(18)

and the lattice parameters determined in this investigation were a_o = 2.879Å, b_o = 5.824Å, c_o = 4.868Å and a monoclinic angle γ = 91.33 . The x-ray pattern exhibited a number of faint additional lines that could not be indexed on the basis of the monoclinic structure. These are listed in Table 2 and tentatively assigned to an omega-type phase analogous to that observed in Ti or Zr base alloys as well as alloys of uranium with Ti or Zr (15-17). These lines were relatively broad suggesting that in the quenched state, this phase exists in a form analogous to that of the "diffuse" omega in more highly alloyed Ti or Zr base alloys. As in the Ti or Zr alloys, this form of omega exerts essentially no influence on strength. This is indicated by the relatively low hardness (R_c20) of the as-quenched 905 alloy.

Isothermal Transformation of the 1.5% Quaternary Alloy

Hardness, dilatometric and metallographic techniques were employed to determine the TTT diagram for the 1.5% quaternary alloy. Isothermal hardness curves for samples quenched to the reaction temperature from 1650°F (900°C) are presented in Fig. 4. Hardening is quite rapid at virtually all temperatures and the peak hardnesses attained are relatively high. The maximum hardness of approximately 55RC was attained at 900°F and this temperature also develops the maximum hardness in the shortest

ageing time. The reaction kinetics are best summarized in the TTT curve obtained from the hardness and metallographic studies and presented in Fig. 5. Decomposition of the γ phase takes place at distinctly different rates at temperatures above and below M_S as is evident in the hardness curves presented in Fig. 4 and the distinct C curves in Fig. 5. Although the separate C curves in these quaternary alloys clearly appear to be associated with the martensite reaction, it should be noted that separate reactions characterizing decomposition at high and at low temperatures also occur in more concentrated alloys where martensite formation does not occur at temperatures above the ambient (20).

At temperatures between the A_3 and the A_1, an acicular form of α_N' develops by a nucleation and growth process as shown in Fig. 6. The platelets nucleate preferentially at grain boundaries and inclusions and grow slowly at a rate presumably controlled by diffusion of solute in the matrix. Complete decomposition of the matrix does not occur in this two-phase region and regions of the enriched γ phase are clearly evident in Fig. 6. Extending the transformation time to one week did not significantly change the amount of untransformed γ. The hardening associated with transformation at 1150°F is relatively small and microhardness measurements indicated

that hardening occurred primarily in the matrix. The relatively coarse plates of α'_N evidently restrict the hardness rather severely.

The structural changes that occur at this and all other temperatures are quite complex. Diffraction patterns exhibit many additional lines and, unfortunately, the principal phases that form have many reflections in common. The d spacings for some of the principal phases expected in these alloys are assembled in Table 3. These data have been used for a tentative identification of the principal phases that form in these alloys; however, the patterns of U_2Ti, UZr_2 and omega are so similar that, in general, no attempt was made to distinguish between these phases. In addition, U_2Mo and γ_d^o are sufficiently similar that it was deemed inadvisable to distinguish between these phases until more detailed studies can be undertaken.

X-ray studies (Table 4) indicate that the acicular precipitate that forms at 1150°F has the orthorhombic α' structure, but many additional lines are present. Comparison with Table 2 for the as-quenched structure reveals clearly the disappearance of the monoclinic structure even at this relatively short ageing time of 500 seconds, and this is confirmed by the absence of the banded martensitic structure in the matrix (Fig. 6A).

The matrix hardening produced at 1150°F appears to be associated with the formation of transition phases consisting primarily of omega but possibly also some γ_d^o. The omega reflections are split; however, detailed interpretation of this is not yet possible. Although the split reflections correspond approximately with those for U_2Ti and UZr_2, it is equally possible that the split reflections result from the formation of omega of different compositions corresponding to an enriched γ surrounding α_N' plates and a γ with the average composition of the untransformed matrix. As shown in Table 5, long reaction times yield the intermediate phases U_2Ti and U_2Mo and it appears that this may be accomplished by ordering of solute within the transition phases. These phases could not be revealed metallographically, and an extensive transmission electron microscopy study would be required to explore these reaction sequences in greater detail.

Although the reactions that occur at temperatures between the M_s and A_1 are basically the same as those at 1150°F, the α_N' phase develops with a distinctly different morphology and distribution. This appears to be the primary factor responsible for the substantially greater hardness that develops at reaction temperatures below A_1 compared with that produced at 1150°F. That is, formation of α_N' at all reaction temperatures constitutes

an overageing reaction that reduces hardness.

The evolution of the microstructure at 1000°F is shown in Fig. 7 and Tables 6 and 7 present x-ray data. Although the banded structure is evident in the matrix at the shortest reaction times (Fig. 7a) the ability to reveal this structure metallographically was lost relatively rapidly (Figs. 7b and 7c). Additional diffraction lines characteristic of the γ_d^o and ω phases accompanied this microstructural change as in the reactions at 1150°F. Thus, it appears that the matrix undergoes a rather uniform decomposition to a complex structural state involving the transition phases.

The distribution of the α_N' phase is the primary metallographic distinction between the reactions at 1000 and 1150°. In particular, the large acicular platelets of alpha that form at 1150°F are not observed at 1000°F. Rather, as shown in Figs. 7b and 7c, α_N' forms as small particles along twin bands that have developed in the matrix and to a lesser extent at grain boundaries. Thus, although this temperature is above M_s, it appears that the banded structure existed at the reaction temperature and formed as an integral part of the sequence involving the transition phases.

The parameters of the α' phase gradually approach those of pure uranium as the reaction time is extended

(Table 8). As shown in Tables 6 and 7 the patterns characterizing the transition or intermediate phases also adjust slowly as the reaction proceeds. Although the parameter changes of the α' phase undoubtedly reflect its changing composition by precipitation of the intermediate phases, it is not possible to decide from these results whether the intermediate phases form by ordering within transition phases of the ω and γ_d^o type or whether the U_2Ti and U_2Mo nucleate independently forcing the transition phases to redissolve as the intermediate phases evolve. Regardless of the detailed mechanisms of these precipitation reactions, it appears that these reactions are the primary source of the hardening observed in these alloys.

As shown in Figs. 4 and 5 transformation initiates much more rapidly at temperatures below M_s than it does at higher temperatures. In particular, the pronounced induction period that precedes hardening at temperatures above M_s is essentially absent at 700°F. In addition, hardening below M_s follows a different time law than that above M_s as is evident from the forms of the reaction curves in the two temperature ranges. X-ray data, presented in Tables 9 to 12, indicate that the monoclinic martensite α'' is converted to the orthorhombic form α' at relatively short ageing times (Table 10) and the transition and intermediate phases form here as in the higher

temperature range. Apparently these transition phases can form either from the BCC or martensitic phases although the kinetic data suggest higher nucleation rates in the latter case.

The hardness data indicate that overageing is severely retarded at temperatures below M_s and metallographic data appear to support this observation. In particular, as shown in Fig. 8, there are few indications of the α'_N phase. Although the ageing reactions have obliterated the banded structure characteristic of the monoclinic martensite, there are no clearly defined indications of the α'_N phase. Subboundaries are delineated in the matrix, however, which may signify initiation of this overageing reaction.

The parameters of the α structure are presented in Table 13. As at the higher temperature (Table 8) the parameters of the α phase gradually approach those of pure uranium again suggesting a slow adjustment in composition associated with the precipitation reactions.

Quench-Ageing Response

The ageing response of quenched alloys was examined only briefly in this study for comparison with the isothermal data. Fig. 9 presents hardness as a function of time at several reaction temperatures. These data are in general agreement with those reported by Colling and

Greenspan(18). Comparison of Figs. 4 and 9 indicates that the ageing reactions occur much more rapidly than the isothermal response. However, the maximum hardness achieved by ageing was comparable with that obtained by isothermal transformation.

It is evident in Fig. 9 that overageing did not occur at 800°F or lower temperatures at the longest times examined. Overageing did occur at 1000°F and, as in the isothermal treatments, was associated with formation of an incoherent α phase. However, the nature of this reaction was significantly different in the aged compared to the isothermally transformed treatments.

Fig. 10 illustrates the sequence of structural changes produced by ageing at 1000°F. The banded structure evident in Fig. 10A suggests that martensite did not revert to γ on heating to the reaction temperature and it is apparent that a cellular product has nucleated at the grain boundaries. Microhardness readings obtained on the matrix and on the cellular product are reported in Table 14. The cellular product exhibits an intermediate hardness of 400 DPH; however, the matrix hardens rapidly. Thus, as in the isothermal studies, precipitation reactions on a fine scale within the matrix are responsible for the hardening and the cellular reaction induces overageing. X-ray studies again revealed many extra diffraction

lines characteristic of the transition and intermediate phases.

At longer ageing times, subtle changes occur within the cellular product - Figs. 10 C and D. As in other uranium-base alloys (13, 21) a secondary change analogous to the recrystallization reaction in other age-hardening systems occurs within the cellular structure. This reaction leads to a significant coarsening of the structure and yields resolvable precipitates probably of U_2Ti (Fig. 10D). It is the initiation of this secondary reaction that is responsible for the renewed softening after long ageing times at 1000°F (Fig. 9). The significant structural difference produced by ageing (Fig. 10) as compared to isothermal transformation (Fig. 7) suggests the the two heat-treating procedures should yield significantly different mechanical properties. Since structures analogous to that produced isothermally should occur in continuous cooling treatments of massive sections, an evaluation of the mechanical behavior of the isothermally transformed structures would be of value.

At ageing temperatures of 800°F and below, these alloys are quite resistant to overageing. As shown in Fig. 11, this results from the absence of the cellular reaction or other incoherent forms of the alpha phase. The ageing response at 600°F is particularly interesting

and exhibits a double ageing response. X-ray studies of Colling and Greenspan (18) have shown that the monoclinic structure of the as-quenched martensite is converted to the orthorhombic structure at ageing times as short as 0.1 hours and that, as in the isothermal reactions, the parameters of the α_b' phase gradually adjust toward those of pure uranium. Thus, it appears that the initial, very rapid hardening, is associated primarily with conversion of the monoclinic to the orthorhombic structure and it seems most likely that the continued hardening reflects precipitation reactions analogous to those observed in the isothermal treatments.

Isothermal Transformation of the 3/4% Quaternary Alloy

The results of a preliminary study of isothermal transformation of the 3/4% quaternary alloy are presented in Figs. 12 and 13. The dilatometric studies indicated that the critical temperatures of this alloy were only slightly higher than those for the 905 alloy. The A_1 and A_3 temperatures for the 904 alloy are 1150°F (627°C) and 1230°F (677°C) respectively.

As previously demonstrated by Tardif[1], the hardness of the as-quenched 904 alloy was substantially higher than that of the 905 alloy. Comparison of Figs. 4 and 13 also reveals that transformation occurs more rapidly in the 904 than in the 905 alloy; however, the maximum

hardness attained by isothermal transformation was somewhat less for the 904 alloy compared to that for the 905. Although x-ray diffraction data are not available for the 904 alloy, it seems most likely that the hardening reactions again occur primarily in the matrix and are associated with the precipitation of the transition and intermediate phases as in the 905 alloy.

Metastable States in Uranium Alloys

The propensity of uranium-base alloys to form metastable transition phases during transformation appears to be intimately connected with the range of martensitic structures that develop depending on cooling rate and alloy content. The effect of alloy content has been discussed by Jackson (22) for the uranium-niobium system and similar results have been obtained for many uranium alloys (6, 8, 9, 23-25). Fig. 14 presents a schematic representation indicating that the γ phase transforms successively during quenching to the tetragonal γ_d^o, monoclinic α'' and orthorhombic α' phases. These transitions are completely reversible and take place in a martensitic, diffusionless manner.

In spite of the martensitic character of these reactions, structural details as well as transformation temperatures vary slightly with cooling rate (6, 22-24).

This effect of cooling rate on the α_b'' phase also was observed in the present study. Specifically, Table 15 compares the lattice parameters of the α'' martensite in the 905 alloy observed in this investigation with those reported by Colling and Greenspan (18). The most significant difference in these values is that for the monoclinic angle γ. The initial water-quenched sample in this investigation was wrapped in molybdenum foil and vacuum encapsulated. Quenching of this sample by breaking the capsule under water resulted in an angle γ of 92.6° similar to that reported by Colling and Greenspan. An unwrapped sample quenched in iced brine yielded an angle of 91.33° (Table 15). Thus, it is apparent that the monoclinic structure is quite sensitive to cooling rate. As suggested by Tangri and co-workers (6, 26), this influence of cooling rate on the martensitic structures appears to be intimately connected with the magnitude of the quenching stresses. Thus, more severe quenching yields structures closer to that of α-uranium as reflected in the reduction of the monoclinic angle.

Although there can be little doubt regarding the importance of quenching stresses in these transformations, the transformations themselves arise from the stability of the parent phase to displacement waves. The sequence

of martensitic structures observed in uranium alloys has been discussed in these terms (27) and, in particular, has been related to the stability of each of the structures to tranverse [110] and [112] vibrational modes. Similar successive martensitic transformations occur in a number of systems and have been shown to result from successive operation of specific vibrational modes.

While the γ_d^o structure results from the stability toward a [110] [001] vibrational mode (27) the omega structure results from the 2/3 [112] [$\bar{1}\bar{1}1$] mode (28, 29) and this structure has been reported in U-Ti and U-Zr alloys.

In the context of the present investigation, the importance of these considerations is related to the matrix hardening and its correlation with formation of the transition phases. Lattice instability can result in either a martensitic structure or in a modulated structure consisting of an intimate mixture on a submicron scale of the transition phase and the parent. The latter may be either the BCC γ phase or one of the martensitic variants of the α phase. The critical condition deciding whether a martensitic or a modulated structure develops is not yet fully understood but appears to be intimately related to the ability to generate the mobile interface that produces the lattice invariant strains of the martensitic reaction.

The interfaces associated with the banded martensitic structure in these alloys are highly mobile and this appears to be one of the major reasons for the low strength and hardness of these martensitic structures (13). Formation of the transition structure in a modulated arrangement within the martensitic structure, on the other hand, should lock the interfaces and interfere with slip within the martensitic structure. This appears to be the primary reason for the matrix hardening observed in both the isothermal and quench-ageing treatments.

REFERENCES

1. Tardif, H.P., "The Heat-Treatability and Properties of Uranium Alloys", Can. Mining Metal. Bull., 58 (1965), 1167.

2. Greenspan, J.,and Rizzitano, F.J., "Development of a Structural Uranium Alloy", Army Materials Research Agency, Watertown, Mass., Report No. AMRA-TR-64-28, September 1964.

3. Tardif, H.P., "A Study of Polynary Uranium Mo-Zr-Nb-V Alloys", Can. Mining Metal. Bull., 61 (1968), 1289.

4. Wolf, S.M., and Rizzitano, F.J., "Properties of Several Structural U-Mo-Cb-V-Ti Alloys", Army Materials Research Agency, Watertown, Mass., Report No. AMRA-TR-67-18, June 1967.

5. Brook, G.B., "Transformation Characteristics of Quaternary Uranium Alloy Containing Molybdenum, Niobium and Zirconium", U.S. Atomic Energy Commission on the Physical Metallurgy of Uranium Alloys. Vail, Colorado, February 12-14, 1974.

6. Tangri, K., and Williams, G.I., "Metastable Phases in the Uranium-Molybdenum System and Their Origin", J. Nucl. Mater., 4 (1961), 226.

7. Hills, R.F., Howlett, B.W., and Butcher, B.R., "Further Studies on the Decomposition of the Gamma Phase in Uranium-Low Molybdenum Alloys", J. Less-Common Metals, 5 (1963), 369.

8. Howlett, B.W., "A Study of the Shear Transformation from the Gamma-Phase in Uranium-Molybdenum Alloys Containing 6.0-12.5 at % Molybdenum", J. Nucl. Mater., 35 (1970), 278.

9. D'Amato, C., Saraceno, F.S., and Wilson, T.B., "Phase Transformations and Equilibrium Structures in Uranium-Rich Niobium Alloys", J. Nucl. Mater., 12 (1964), 291.

10. Kishineuskii, J.B., Tret'Yakov, A.A., Gomozov, L.I. and Ivanov, O.S., "Kinetics of the Isothermal Transformation of Gamma Solid Solutions of Some Uranium Alloys", Translated from the Russian for the University of California, Lawrence Radiation Laboratory, Livermore. U.S. Atomic Energy Commission Report No. UCRL-Trans-10452, March 1970.

11. Justusson, W.M., "Transformation Kinetics of Gamma-Phase Uranium-Molybdenum-Niobium Alloys", J. Nucl. Mater., 4 (1961), 37.

12. Peterson, C.A.W., Steele, W.J., and DiGiallonardo, S.L., "Isothermal Transformation Study of Some Uranium-Base Alloys", University of California, Lawrence Radiation Laboratory, Livermore. U.S. Atomic Energy Commission Report No. UCRL-7824, August 1964.

13. Eckelmeyer, K.H., "Aging Phenomena in Dilute Uranium Alloys", U.S.Atomic Energy Commission Conference on the Physical Metallurgy of Uranium Alloys. Vail, Colorado, February 12-14, 1974.

14. Lehmann, J., and Hills, R.F., "Proposed Nomenclature for Phases in Uranium Alloys", J. Nucl. Mater., 2 (1960), 261.

15. Tomlinson, R.D., Silcock, J.M., and Burke, J., "The Isothermal Decomposition of Gamma-Phase Uranium-Titanium Alloys", J. Inst. Metals, 98 (1970), 154.

16. Hatt, B.A., "The Orientation Relationship Between the Gamma and Alpha Structures in Uranium-Zirconium Alloys", J. Nucl. Mater., 19 (1966), 133.

17. Silcock, J.M., "Intermediate Phase in the Uranium-Zirconium System", Trans. AIME, 207 (1957), 521.

18. Colling, D.A., and Greenspan, J., "Polynary Uranium Alloys", U.S. Atomic Energy Commission Conference on the Physical Metallurgy of Uranium Alloys. Vail, Colorado, February 12-14, 1974.

19. Droplet, J.P., "A Review of DREV Uranium Research", U.S. Atomic Energy Commission Conference on the Physical Metallurgy of Uranium Alloys. Vail, Colorado, February 12-14, 1974.

20. Repas, P.E., Goodenow, R.H., and Hehemann, R.F., "Transformation Characteristics of Three Uranium Base Alloys", Case Institute of Technology, Cleveland, Ohio. Report No. AMRA CR 63-02/1(F). January 1963.

21. Ammons, A.M., "Precipitation Hardening in Uranium-Rich Uranium Alloys", Union Carbide Corp., Y-12 Plant, Oak Ridge, Tenn., U.S. Atomic Energy Commission Preprint Y-DA-5353, December 1973.

22. Jackson, R.J., "Reversible Martensitic Transformations Between Transition Phases of Uranium-Base Niobium Alloys", Dow Chemical Company, Rocky Flats Division, Golden, Colorado. U.S. Atomic Energy Commission Report No. RFP-1535, December 1970.

23. Jackson, R.J., and Larsen, W.L., "Transformations and Structures in the Uranium-Rhenium System", J. Nucl. Mater., 21 (1967), 263.

24. Anagnostidis, M., Colombie, M., and Monti, H., "Metastable Phases in Uranium-Niobium Alloys", J. Nucl. Mater., 11 (1964) 67.

25. Tangri, K., and Chaudhuri, D.K., "Metastable Phases in Uranium Alloys with High Solute Solubility in the BCC Gamma Phase. Part I - The System U-Nb", J. Nucl. Mater., 15 (1965), 278.

26. Tangri, K., "Les Phases Gamma Metastables dans les Alliages d'Uranium Contenant du Molybdene", Mem. Sci. Rev. Met., 58 (1961), 469.

27. Blake, D., and Hehemann, R.F., "Transformations in Uranium-Base Alloys", U.S. Atomic Energy Commission Conference on the Physical Metallurgy of Uranium Alloys. Vail, Colorado, February 12-14, 1974.

28. Defontaine, D., "Mechanical Instabilities in the BCC Lattice and the Beta to Omega Phase Transformation", Acta Met., 18 (1970), 275.

29. Cook, H.E., "On the Nature of the Omega Transformation", Acta Met., 21 (1973), 1445.

30. Yakel, H.L., "Crystal Structures of Transition Phases Formed in U-16.6 at % Nb-5.64 at %Zr Alloys), J. Nucl. Mater., 33 (1969), 286.

31. Halteman, E.K., "The Crystal Structure of U_2Mo", Acta Cryst., 10 (1957), 166.

32. Knapton, A.G., "The Crystal Structure of U_2Ti", Acta Cryst., 7 (1954), 457.

33. Boyko, E.R., "The Structure of the δ Phase in the Uranium-Zirconium System", Acta Cryst., 712.

34. Jacobs, C.W., and Warren, B.E., "The Crystalline Structure of Uranium", J. Am. Chem. Soc., 59 (1937), 2588.

TABLES

TABLE 1

CHEMICAL COMPOSITIONS*

Alloy	Mo	Nb	Zr	Ti	V
904	0.75	0.82	0.72	0.49	0.06
905	1.52	1.46	1.45	0.49	0.07

Alloy	C	O(ppm)	H(ppm)	N(ppm)
904	0.03	31	3.0	24
905	0.01	47	3.9	7

*Listed as weight percent unless otherwise noted.

TABLE 2

X-RAY DATA - 905 ALLOY

BRINE QUENCHED FROM 1650°F (900°C)
DIFFRACTOMETER PATTERN

2θ	d(OBS)Å	I	Phase	2θ	d(OBS)Å	I	Phase
21.31	4.1694	90	ω	75.73	1.2559	90	221α''
31.02	2.8829	180	020α''	76.10	1.2508	110	042α''
33.60	2.6672	90		76.43	1.2462	120	ω
33.95	2.6405	100		77.04	1.2378	90	221α''
34.30	2.6103	170	$\bar{1}$10α''	78.24	1.2217	60	004α''
34.70	2.5851	460		79.32	1.2079	60	ω
35.10	2.5566	460	110α''	83.52	1.1575	70	ω
36.05	2.4913	Off-scale	021α''	84.17	1.1502	70	222α''
37.10	2.4232	110	002α''	86.95	1.1204	70	ω
39.23	2.2964	330	$\bar{1}$11α''	92.32	1.0688	70	150α''
40.00	2.2540	110	111α''	92.58	1.0665	70	ω
45.50	1.9935	70	γ	96.37	1.0343	60	$\bar{2}$40α''
46.72	1.9442	70	ω	98.10	1.0207	80	ω
47.44	1.9164	70	020α''	98.62	1.0167	70	$\bar{2}$23α''
51.07	1.7884	160	$\bar{1}$12α''	99.46	1.0103	80	240α''
51.30	1.7809	140	ω	100.30	1.0039	60	ω
56.80	1.6208	70	$\bar{1}$30α''	101.74	.9938	70	$\bar{1}$52α''
57.71	1.5974	70	130α''	102.00	.9920	70	223α''
59.95	1.5436	80	$\bar{1}$31α''	102.18	.9907	70	241α''
60.27	1.5355	110	ω	108.28	.9511	80	061α''
61.24	1.5135	100	131α''	108.82	.9480	80	ω
64.69	1.4409	280	200α''	109.53	.9438	90	310α''
66.52	1.4056	70	023α''	111.31	.9337	70	044α''
67.13	1.3943	90	041α''	112.17	.9289	70	ω
69.30	1.3559	90	132α''	127.71	.8588	60	243α''
72.53	1.3033	60	ω	128.56	.8557	70	$\bar{3}$31α''

TABLE 3

DIFFRACTION DATA ON TRANSITION PHASES
AND INTERMETALLIC COMPOUNDS

d Spacing - Å			
γ_d^o(30)	U_2Mo(31)	U_2Ti(32)	UZr_2(33)
4.948	4.915	4.18	4.28
3.499	3.237	2.85	3.05
3.371	2.422	2.41	2.49
2.786	2.372	2.35	2.16
2.474	2.174	2.09	1.94
2.428	1.714	1.84	1.77
2.213	1.641	1.69	1.64
1.995	1.516	1.58	1.54
1.850	1.389	1.42	1.45
1.749	1.359	1.39	1.31
1.686	1.230	1.38	1.25
1.649	1.212	1.35	1.20
1.595	1.186	1.25	1.16
1.565	1.084	1.22	1.12
1.553	1.082	1.21	1.06
	1.043	1.18	1.02
	.914	1.16	1.00
		1.11	.97
		1.07	
		1.06	

TABLE 4

X-RAY DATA - 905 ALLOY

ISOTHERMALLY TRANSFORMED AT 1150°F (621°C) FOR 500 Sec.

POWDER CAMERA PATTERN

θ	d(OBS)Å	I	Phase	θ	d(OBS)Å	I	Phase
10.63	4.1783	W	ω	32.49	1.4356	M	$200_{\alpha'}$
10.93	4.0659	M		33.65	1.3913	W	$041_{\alpha'}$
11.83	3.7605	M		38.31	1.2436	M	$221_{\alpha'}$
12.13	3.6692	M	γ_o				
13.85	3.2201	VW	ω	41.95	1.1532	VW	$133_{\alpha'}$
14.30	3.1211	VVW	ω	42.45	1.1421	VW	$222_{\alpha'}$
17.73	2.5317	VW	$110_{\alpha'}$	43.65	1.1168	W	$144_{\alpha'}$
18.20	2.4685	S	$002_{\alpha'}$	45.87	1.0741	VVVW	$042_{\alpha'}$
19.86	2.2694	M	$111_{\alpha'}$				
				49.55	1.0131	VVVW	γ_o
23.45	1.9369	S	ω	51.30	.9878	VVW	$152_{\alpha'}$
24.85	1.8342	W	ω γ	51.75	.9817	VVW	$134_{\alpha'}$
25.69	1.7779	M	$112_{\alpha'}$	55.00	.9410	MW	$310_{\alpha'}$
27.70	1.6865	M	γ_o, ω	56.15	.9282	VVVW	$115_{\alpha'}$
28.82	1.5990	VW	$130_{\alpha'}$	65.72	.8457	VVVW	$135_{\alpha'}$
30.16	1.5344	W	$131_{\alpha'}$	68.27	.8299	VVVW	$006_{\alpha'}$
30.78	1.5065	W	ω	71.00	.8153	VVW	$313_{\alpha'}$
				77.92	.7883	VW	γ_o

TABLE 5

X-RAY DATA - 905 ALLOY

ISOTHERMALLY TRANSFORMED AT 1150°F (621°C) FOR 10,000 SEC.

DIFFRACTOMETER PATTERN

2θ	d(OBS)Å	I	Phase	2θ	d(OBS)Å	I	Phase
32.50	2.7549	70	U_2Ti	99.09	1.0131	60	223α'
35.10	2.5629	80	110α'	101.05	.9987	60	241α'
39.10	2.3037	170	111α'	101.93	.9925	130	152α'
48.15	1.8898	90	022α'	108.98	.9470	100	U_2Ti
51.22	1.7835	250	112α'	109.31	.9451	100	004α'
53.37	1.7166	120	U_2Mo	109.45	.9443	100	242α'
56.72	1.6229	70	U_2Mo	110.35	.9391	110	310α'
57.23	1.6097	160	130α'	110.65	.9374	90	025α'
60.45	1.5314	90	131α'	111.00	.9354	70	204α'
65.00	1.4348	70	023α'	112.95	.9247	80	U_2Ti
65.39	1.4272	70	200α'	113.40	.9223	70	331α'
65.52	1.4246	70	U_2Ti	114.21	.9181	70	U_2Ti
67.23	1.3925	70	U_2Mo	115.10	.9135	70	U_2Mo
67.50	1.3876	60	U_2Ti	115.70	.9105	60	062α'
76.71	1.2423	210	211α'	121.23	.8847	60	U_2Ti
76.93	1.2393	210	U_2Ti	122.48	.8794	60	U_2Mo
83.92	1.1530	80	133α'	132.25	.8430	70	135α'
87.20	1.1179	80	U_2Ti	132.59	.8419	70	331α'
89.65	1.0936	60	043α'	141.92	.8155	80	313α'
90.60	1.0846	60	150α'	142.20	.8148	80	154α'
91.22	1.0788	60	U_2Mo	142.67	.8137	70	U_2Ti
96.38	1.0343	60	U_2Mo	144.70	.8041	60	U_2Mo

TABLE 6

X-RAY DATA - 905 ALLOY

ISOTHERMALLY TRANSFORMED AT 900°F (482°C) FOR 100 SEC.
DIFFRACTOMETER PATTERN

2θ	d(OBS)Å	I	Phase	2θ	d(OBS)Å	I	Phase
30.65	2.9168	120	020α'	76.49	1.2453	280	221α'
31.50	2.8400	80	1	76.67	1.2429	290	004α'
34.95	2.5672	Off-scale	110α'	77.15	1.2363	130	202α'
35.73	2.5129	680	021α'	79.50	1.2056	60	2
36.21	2.4807	480	002α'	83.60	1.1566	110	2
37.08	2.4245	270	2	83.84	1.1539	120	133α'
37.22	2.4157	270	1	83.92	1.1530	120	1
38.07	2.3637	110	2	84.65	1.1449	70	024α'
38.70	2.3266	100	2	85.06	1.1404	120	222α'
39.50	2.2813	790	111α'	87.09	1.1190	100	1
43.50	2.0804	70	2	87.33	1.1165	110	114α'
45.15	2.0081	70	1	88.12	1.1086	60	2
48.14	1.8901	100	022α'	90.74	1.0832	70	150α'
51.19	1.7845	610	112α'	98.13	1.0204	130	2
52.23	1.7514	70	2	98.99	1.0147	80	223α'
54.78	1.6757	70	2	100.53	1.0025	90	2
57.21	1.6102	70	1	101.90	.9927	90	2
60.42	1.5321	310	131α'	103.24	.9834	80	134α'
61.68	1.5038	80	1	107.19	.9578	80	2
63.15	1.4723	80	1	108.72	.9486	100	2
63.68	1.4613	120	040α'	109.10	.9463	150	2
64.85	1.4377	230	023α'	109.70	.9428	130	242α'
66.15	1.4126	90	2	110.00	.9411	120	310α'
66.70	1.4023	140	041α'	110.85	.9363	90	204α'
67.38	1.3898	190	1	112.50	.9272	80	2
69.51	1.3523	70	1	114.00	.9192	80	2
75.40	1.2606	80	042α'	117.50	.9017	70	153α'

1. γ_o or U_2Mo

2. ω or U_2Ti

TABLE 7

X-RAY DATA - 905 ALLOY

ISOTHERMALLY TRANSFORMED AT 900°F (482°C) FOR 50,000 SEC.
DIFFRACTOMETER PATTERN

2θ	d(OBS)Å	I	Phase	2θ	d(OBS)Å	I	Phase
34.98	2.5651	200	110α'	99.31	1.0115	70	223α'
39.56	2.2780	760	111α'	99.77	1.0080	70	1
48.18	1.8887	90	022α'	100.77	1.0007	130	2
51.27	1.7819	850	112α'	101.00	.9991	110	223α'
59.39	1.5562	70	2	101.70	.9941	130	2
60.04	1.5409	70	1	102.20	.9906	130	1
60.44	1.5316	110	131α'	102.34	.9896	120	152α'
67.18	1.3934	110	041α'	108.95	.9472	100	2
67.37	1.3899	130	1	109.20	.9457	130	044α'
67.69	1.3842	110	2	109.36	.9448	140	242α'
83.95	1.1527	210	133α'	109.60	.9434	120	025α'
87.23	1.1176	70	2	110.27	.9395	100	130α'
87.40	1.1158	70	114α'	110.45	.9385	90	025α'
90.65	1.0841	80	1	111.00	.9354	80	204α'
91.95	1.0721	130	2	111.30	.9337	70	2
93.50	1.0584	70	2	114.90	.9146	70	1

1. U_2Mo or γ_d^o

2. U_2Ti or ω

TABLE 8

HIGH TEMPERATURE LATTICE PARAMETER COMPARISON - 905 ALLOY. ISOTHERMALLY TRANSFORMED at 900°F (482°C)

	As Quenched	1,000 Sec.	10,000 Sec.	Pure U (34)
a_o	2.879	2.863	2.861	2.852
b_o	5.824	5.832	5.842	5.865
c_o	4.868	4.951	4.963	4.945

TABLE 9

X-RAY DATA - 905 ALLOY

ISOTHERMALLY TRANSFORMED AT 700°F (371°C) FOR 15 SEC.
DIFFRACTOMETER PATTERN

2θ	d(OBS)Å	I	Phase	2θ	d(OBS)Å	I	Phase
20.80	4.2705	130	1	74.14	1.2789	90	$\bar{2}$20α"
21.82	4.0731	130	2	75.23	1.2630	170	$\bar{2}$21α"
24.71	3.6029	120	2	76.25	1.2487	200	2
30.82	2.9011	120	020α"	76.27	1.2422	210	042α"
34.38	2.6084	190	$\bar{1}$10α"	77.21	1.2355	180	1
35.05	2.5601	210	110α"	83.30	1.1600	110	$\bar{2}$
35.95	2.4980	170	021α"	84.22	1.1496	200	$\bar{1}$33α"
36.68	2.4500	120	002α"	85.44	1.1363	160	133α"
37.16	2.4194	120	$\bar{1}$	86.85	1.1215	160	1
39.15	2.3009	250	$\bar{1}$11α"	87.12	1.1187	190	2
39.70	2.2703	460	111α"	88.34	1.1064	110	$\bar{1}$14α"
44.05	2.0557	110	1	89.05	1.0994	100	114α"
49.22	1.8512	100	022α"	89.90	1.0912	100	1
49.95	1.8258	110	$\bar{1}$	93.33	1.0599	90	$\bar{2}$
51.20	1.7841	700	$\bar{1}$12α"	93.52	1.0582	90	$\bar{1}$51α"
52.16	1.7535	140	1	95.38	1.0424	90	151α"
55.82	1.6469	110	2	98.05	1.0211	90	1
56.56	1.6271	170	$\bar{1}$	98.20	1.0199	100	2
56.75	1.6221	170	$\bar{1}$30α"	99.17	1.0215	100	040α"
60.03	1.5411	140	$\bar{1}$31α"	100.82	1.0004	110	2
61.43	1.5093	170	131α"	104.60	.9743	100	2
63.05	1.4744	130	1	106.16	.9643	100	060α"
64.50	1.4417	130	2	107.60	.9553	130	$\bar{3}$10α"
67.34	1.3905	160	041α"	108.40	.9505	130	2
68.31	1.3731	100	113α"	112.09	.9294	120	2

1. U_2Mo or $\gamma_d{}^o$

2. U_2Ti or ω

TABLE 10

X-RAY DATA - 905 ALLOY

ISOTHERMALLY TRANSFORMED AT 700°F (371°C) for 100 SEC.
DIFFRACTOMETER PATTERN

2θ	d(OBS) Å	I	Phase	2θ	d(OBS) Å	I	Phase
30.50	2.9308	220	2	76.12	1.2505	210	2
30.68	2.9140	220	020α'	76.39	1.2467	270	221α'
32.44	2.7599	160	2	76.57	1.2442	250	202α'
34.75	2.5815	170	110α'	77.48	1.2319	120	1
35.67	2.5170	140	021α'	80.64	1.1914	100	2
36.15	2.4887	140	002α'	81.50	1.1810	100	2
38.92	2.3140	150	2	83.55	1.1571	120	2
39.37	2.2886	310	111α'	83.73	1.1551	140	2
41.54	2.1739	120	1	83.89	1.1533	150	133α'
42.20	2.1414	120	2	84.52	1.1463	100	1
44.26	2.0464	120	2	86.77	1.1223	110	2
45.10	2.0102	120	1	87.43	1.1155	110	114α'
48.10	1.8716	130	022α'	89.95	1.0907	130	043α'
49.73	1.8334	120	1	91.08	1.0801	120	150α'
49.83	1.8299	120	2	91.94	1.0722	110	2
51.10	1.7874	450	112α'	93.42	1.0591	100	2
51.74	1.7668	160	2	96.10	1.0365	100	1
53.70	1.7217	150	1	97.50	1.0254	100	240α'
54.77	1.6760	130	2	98.42	1.0182	100	223α'
56.53	1.6279	120	1	100.40	1.0034	120	241α'
57.18	1.6109	130	130α'	100.85	1.0001	120	2
58.08	1.5881	130	1	104.52	.9748	110	2
59.62	1.5484	140	131α'	107.39	.9566	100	2
60.40	1.5325	390	1	110.26	.9396	110	204α'
63.41	1.4669	150	2	110.66	.9373	110	025α'
64.55	1.4437	210	040α'	111.71	.9315	120	311α'
64.84	1.4379	290	023α'	112.04	.9297	140	2
65.95	1.4164	120	2	112.65	.9263	160	115α'
66.43	1.4073	270	1	113.14	.9237	140	2
66.85	1.3995	310	041α'	113.68	.9209	120	2
67.20	1.3930	350	113α'	115.25	.9128	110	2
68.95	1.3619	130	1	117.15	.9034	110	153α'
69.68	1.3494	200	132α'	118.50	.8970	110	2
72.08	1.3103	100	2	121.95	.8816	100	2
75.67	1.2568	120	042α'	126.86	.8619	110	2

1. U_2Mo or γ_d°
2. U_2Ti or ω

TABLE 11

X-RAY DATA - 905 ALLOY

ISOTHERMALLY TRANSFORMED AT 700°F (371°C) for 1000 Sec.
DIFFRACTOMETER PATTERN

2θ	d(OBS)Å	I	Phase	2θ	d(OBS)Å	I	Phase
30.67	2.9150	120	020α'	74.45	1.2743	90	220α'
32.77	2.7328	120	2	76.35	1.2473	120	2
34.92	2.5693	160	110α'	76.65	1.2431	130	004α'
35.72	2.5136	130	021α'	76.82	1.2408	130	221α'
35.84	2.5055	110	2	83.50	1.1577	210	2
36.50	2.4617	120	002α'	83.84	1.1535	280	133α'
37.24	2.4144	120	1	84.85	1.1427	120	024α'
37.70	2.3860	120	2	87.00	1.1199	230	2
38.95	2.3123	120	2	87.18	1.1181	250	114α'
39.52	2.2802	440	111α'	88.19	1.1079	120	2
41.05	2.1987	120	2	100.85	1.0001	130	2
44.39	2.0407	110	2	101.20	.9976	120	241α'
45.40	1.9974	100	1	101.62	.9946	130	2
48.29	1.8846	130	022α'	101.95	.9923	140	2
49.40	1.8448	100	1	102.35	.9895	130	152α'
49.79	1.8313	100	2	107.90	.9535	110	1
51.18	1.7848	470	112α'	108.18	.9518	170	061α'
53.10	1.7247	110	1	108.93	.9473	190	2
53.52	1.7121	110	1	109.18	.9459	190	044α'
56.88	1.6187	110	1	109.82	.9421	200	242α'
57.86	1.5936	110	130α'	110.28	.9395	190	025α'
60.44	1.5316	110	131α'	110.57	.9378	170	310α'
66.43	1.4073	100	2	111.25	.9340	140	2
67.00	1.3967	130	041α'	112.40	.9277	130	115α'
67.10	1.3949	130	113α'	113.00	.9425	130	2
67.50	1.3876	130	1	125.00	.8691	100	243α'
68.80	1.3645	110	2	126.09	.8649	110	2
72.86	1.2982	100	2	127.50	.8595	100	1

1. U_2Mo or γ_d^o

2. U_2Ti or ω

TABLE 12

X-RAY DATA - 905 ALLOY

ISOTHERMALLY TRANSFORMED AT 700°F (371°C) FOR 10,000 SEC.
DIFFRACTOMETER PATTERN

2θ	d(OBSA)Å	I	Phase	2θ	d(OBS)Å	I	Phase
29.36	3.0420	90	2	66.09	1.4137	90	2
30.60	2.9215	110	020α'	66.95	1.3976	110	041α'
31.04	2.8811	100	1	67.26	1.3919	130	113α'
32.75	2.7344	90	2	67.50	1.3876	100	1
34.94	2.5679	160	110α'	68.05	1.3777	90	2
35.82	2.5068	200	021α'	76.48	1.2455	80	221α'
36.15	2.4847	150	002α'	83.37	1.1592	90	2
37.13	2.4213	110	1	84.02	1.1519	150	1
37.68	2.3872	100	2	84.10	1.1510	90	2
39.52	2.2802	320	111α'	87.08	1.1191	100	114α'
47.70	1.9065	80	2	90.55	1.0850	90	1
48.20	1.8879	90	022α'	91.88	1.0728	90	2
51.17	1.7851	180	112α'	101.33	.9987	90	1
51.80	1.7649	90	2	102.18	.9907	120	$152_{\alpha'}$
52.89	1.7310	120	1	107.30	.9572	70	2
53.50	1.7127	160	1	108.68	.9488	120	2
54.83	1.6743	90	2	108.97	.9471	150	2
56.50	1.6287	80	1	109.35	.9449	150	242α'
57.17	1.6112	140	130α'	109.66	.9431	150	025α'
60.44	1.5316	110	131α'	110.31	.9393	100	310α'
63.52	1.4646	90	040α'	112.04	.9297	90	2
64.58	1.4431	110	2	113.06	.9241	100	2
64.81	1.4385	140	220α'	113.45	.9221	80	311α'

1. U_2Mo or γ_d^o

2. U_2Ti or ω

TABLE 13

LOW TEMPERATURE LATTICE PARAMETER COMPARISON -

905 ALLOY. ISOTHERMALLY TRANSFORMED AT 700°F (371°C)

	As Quenched	15 Sec.	100 Sec.	1,000 Sec.	10,000 Sec.	Pure U (34)
a_o	2.879	2.910	2.893	2.860	2.857	2.852
b_o	5.824	5.823	5.832	5.837	5.842	5.865
c_o	4.868	4.874	4.878	4.969	4.969	4.945
γ	91.33°	90.68°	90.00°	90.00°	90.00°	90.00°

TABLE 14

MICROHARDNESS DATA - AGING TRANSFORMATION - 905 ALLOY

Matrix DPH Hardness:

Time (Sec.)	DPH
36	361
180	659
360	855
1800	790

Cellular Product DPH - 402

TABLE 15

α''_b LATTICE PARAMETER COMPARISON

905 ALLOY

	This Investigation	Colling & Greenspan (16)	Pure U (34)
a_o	2.879	2.891	2.852
b_o	5.824	5.842	5.865
c_o	4.868	4.840	4.945
γ	91.33°	92.46°	90.00°

FIGURES

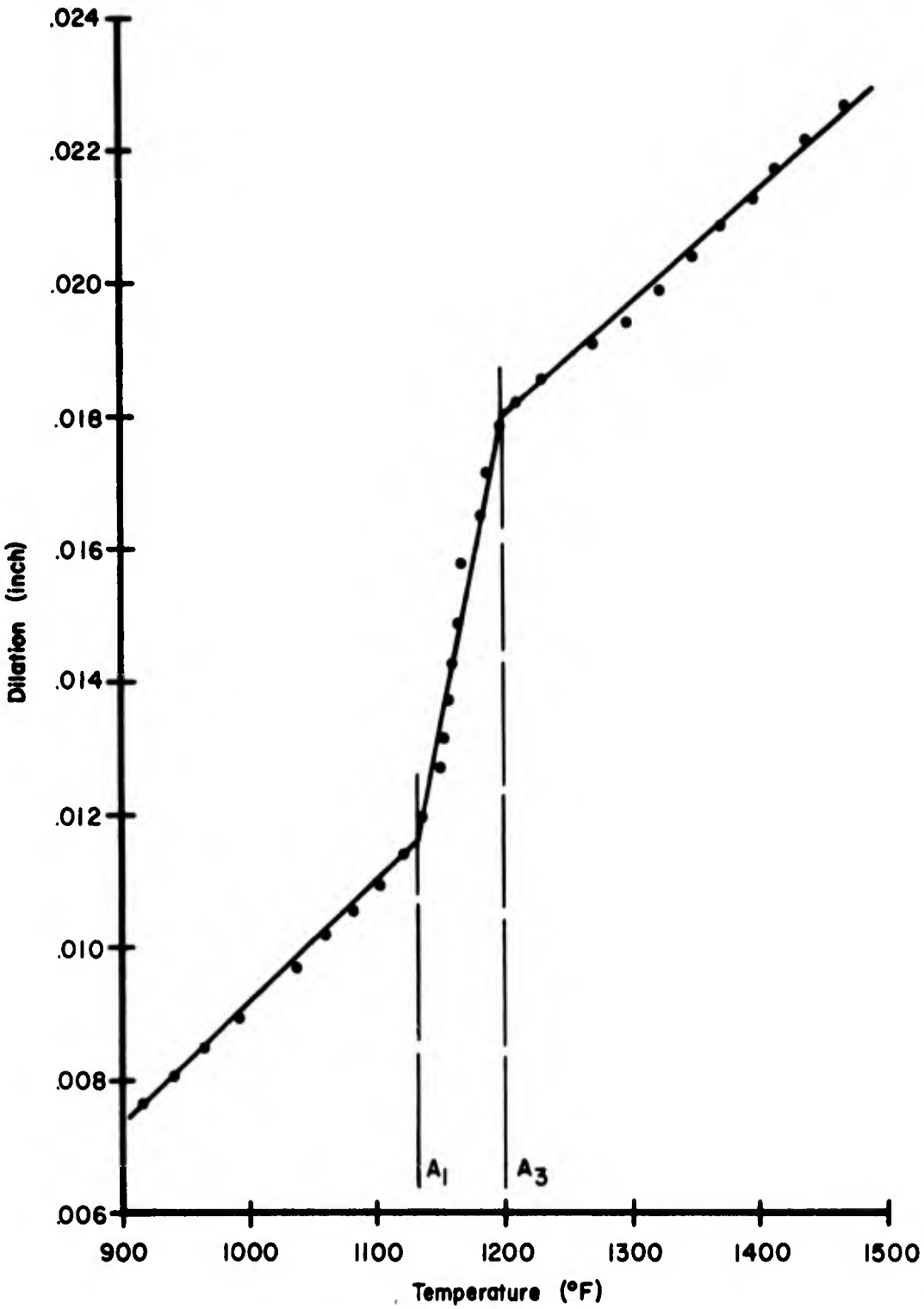

Figure 1. Dilation vs. temperature - fully aged 905 alloy. Slow heating.

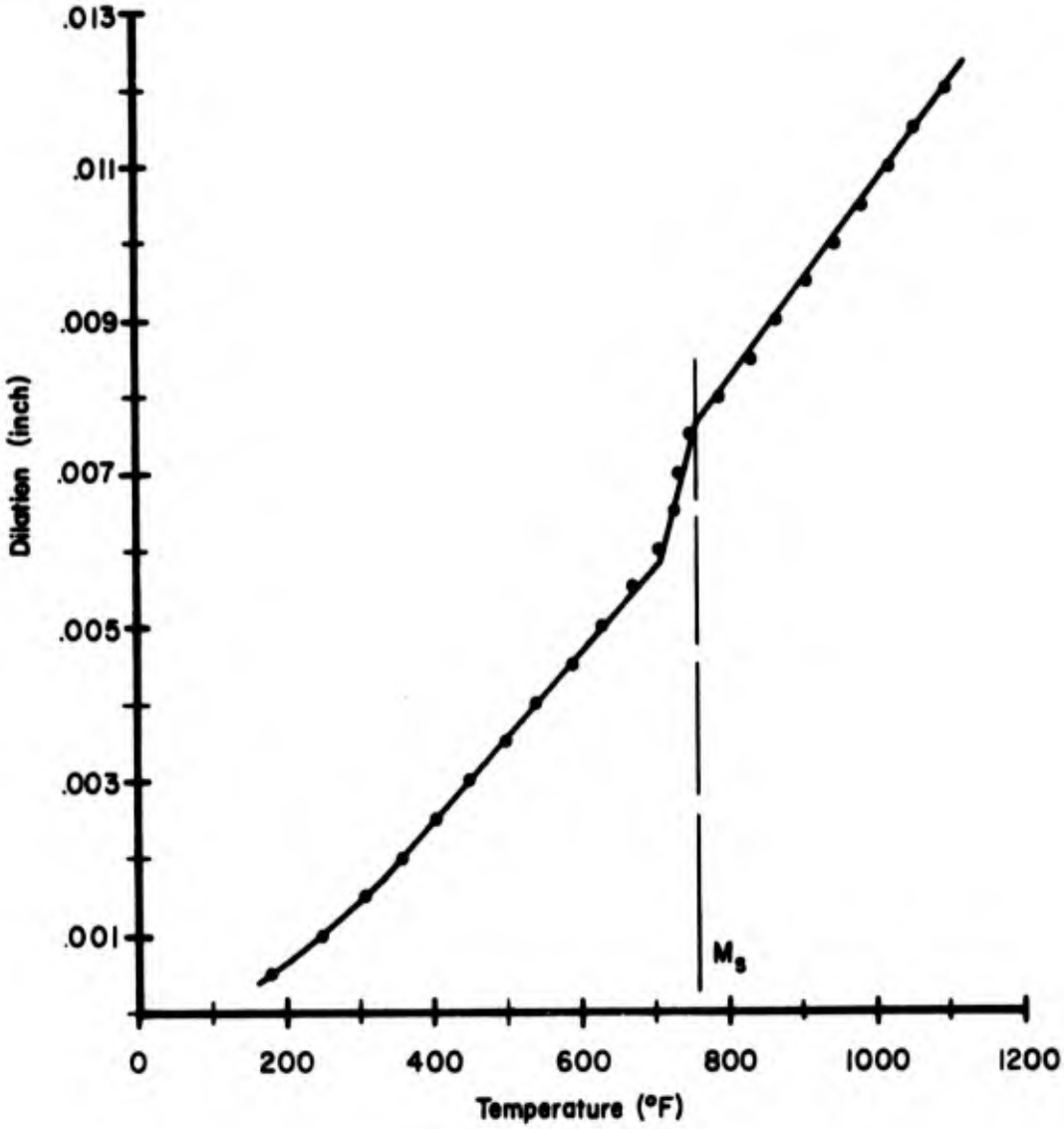

Figure 2. Dilation vs. temperature - homogenized 905 alloy. Air cool.

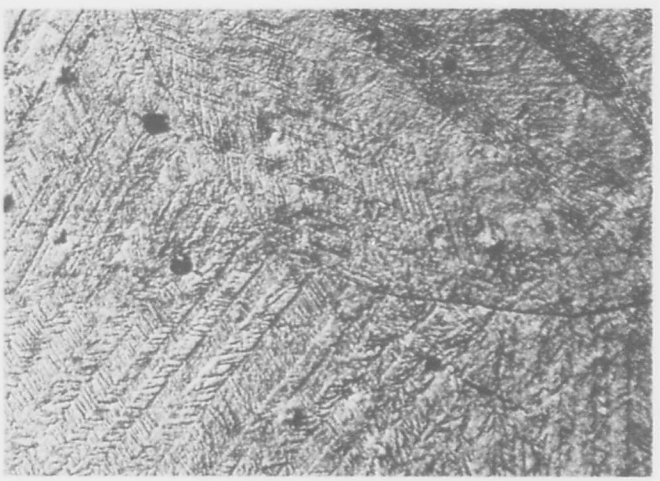

A. 400X.

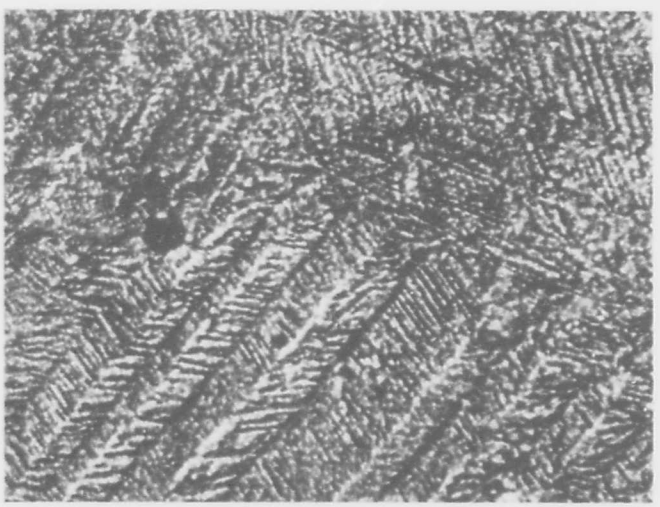

B. 800X.

Figure 3. Structure of the 905 alloy water quenched from 1650°F (900°C).

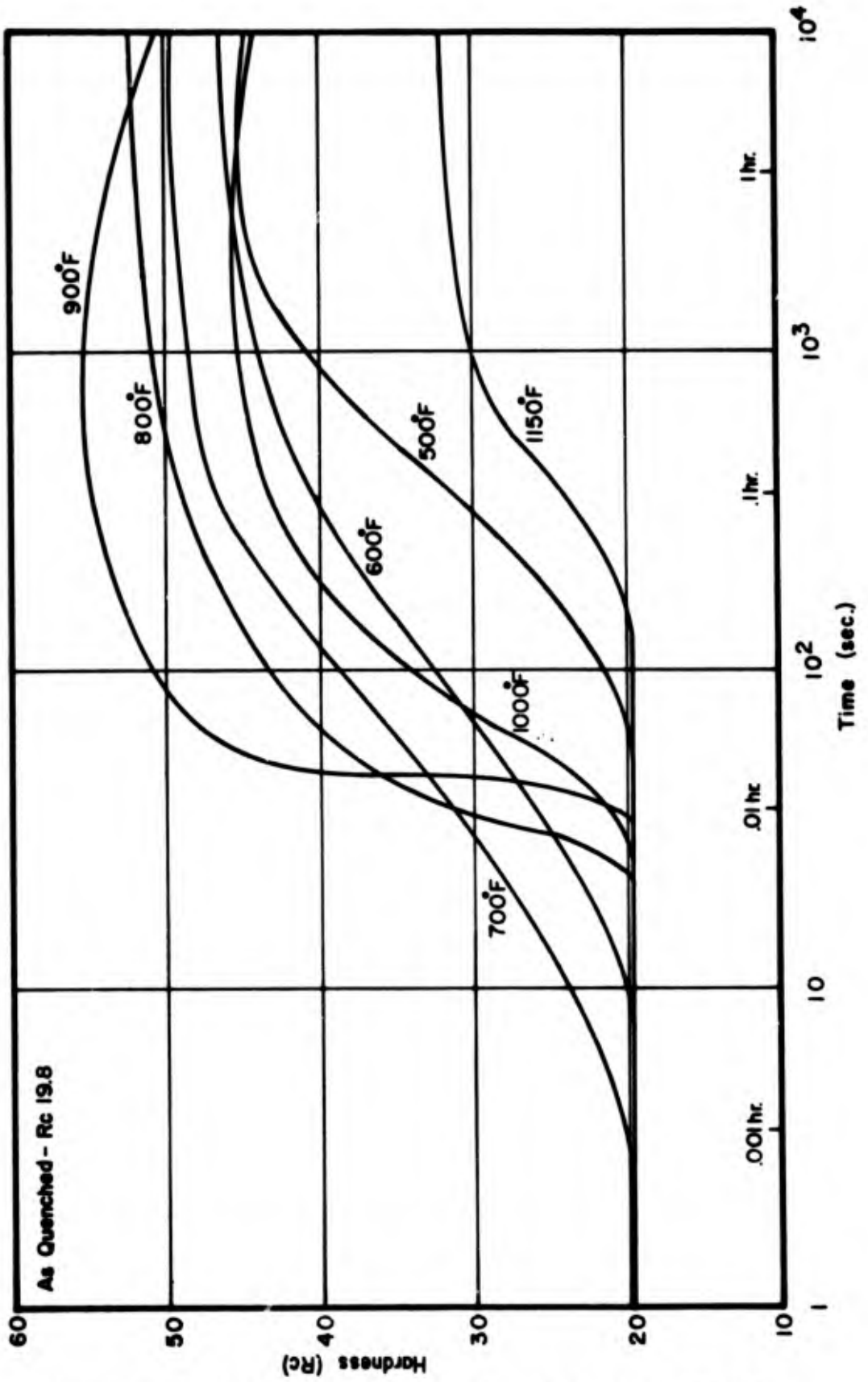

Figure 4. Isothermal transformation hardness - 905 alloy. Quenched to temperature from 1650°F (900°C).

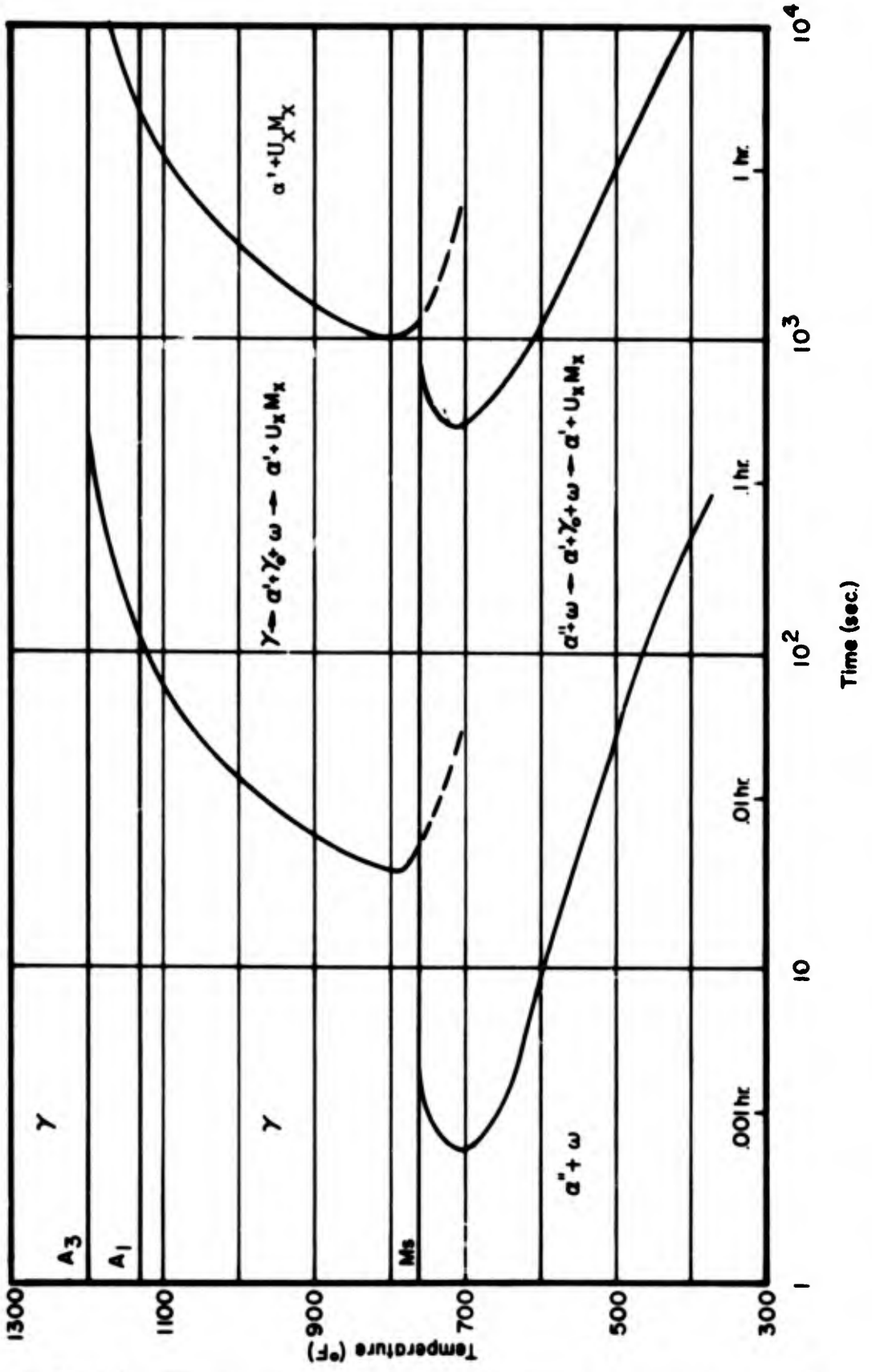

Figure 5. Time - temperature - transformation curve - 905 alloy. Isothermally transformed.

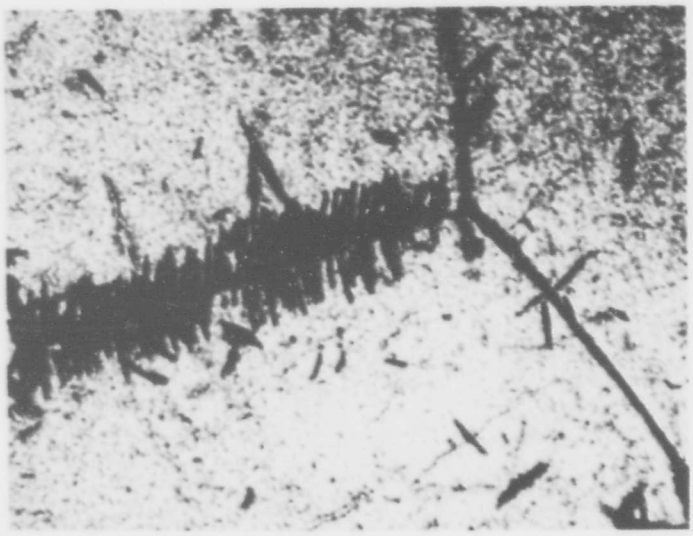

A. 1000 seconds, 800X.

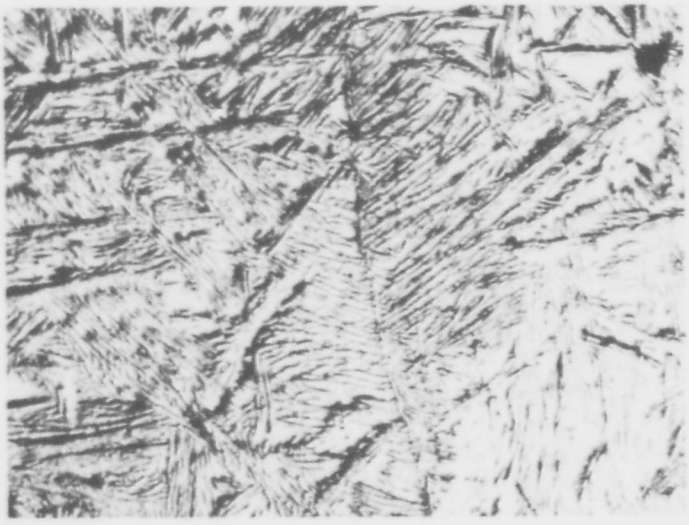

B. 10,000 seconds, 1000X.

Figure 6. Structure of the 905 alloy isothermally transformed at 1150°F (621°C).

A. 10 seconds, 400X.

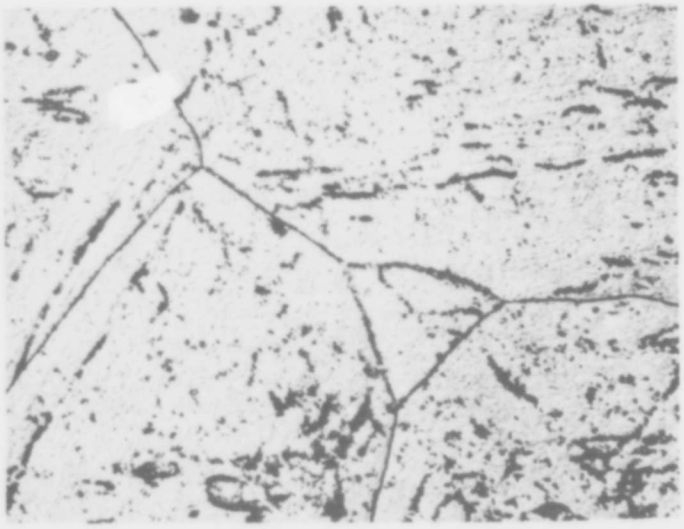

B. 50 seconds, 400X.

Figure 7. Structure of the 905 alloy isothermally transformed at 1000°F (538°C).

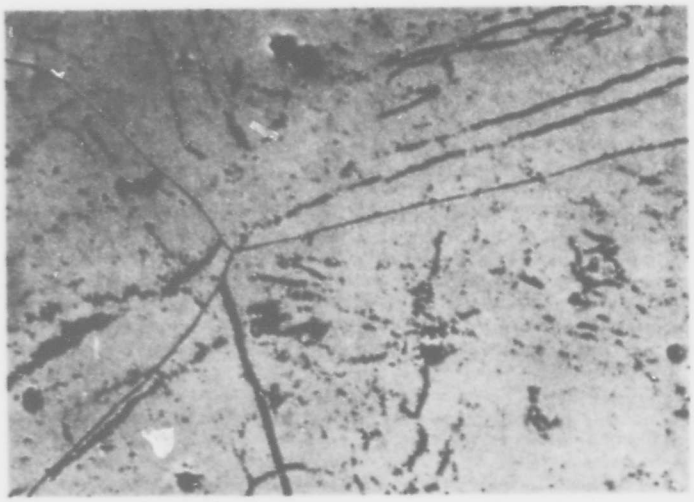

C. 250 seconds, 400X.

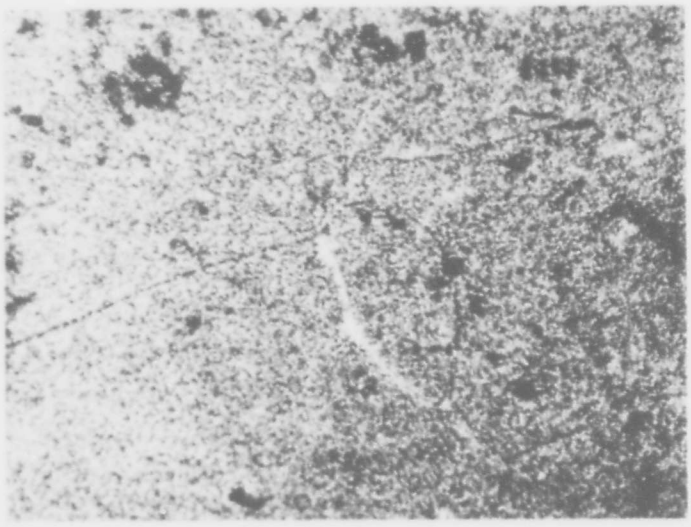

D. 500 seconds, 400X.

Figure 7 (continued). Structure of the 905 alloy isothermally transformed at 1000°F (538°C).

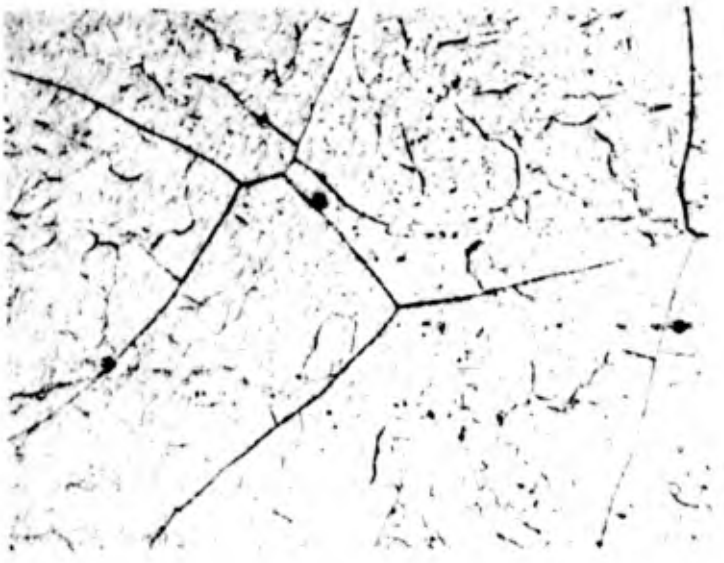

A. 20,000 seconds at 500°F (260°C), 400X.

B. 10,000 seconds at 600°F (316°C), 400X.

Figure 8. Structure of the 905 alloy isothermally transformed at temperatures below the M_s.

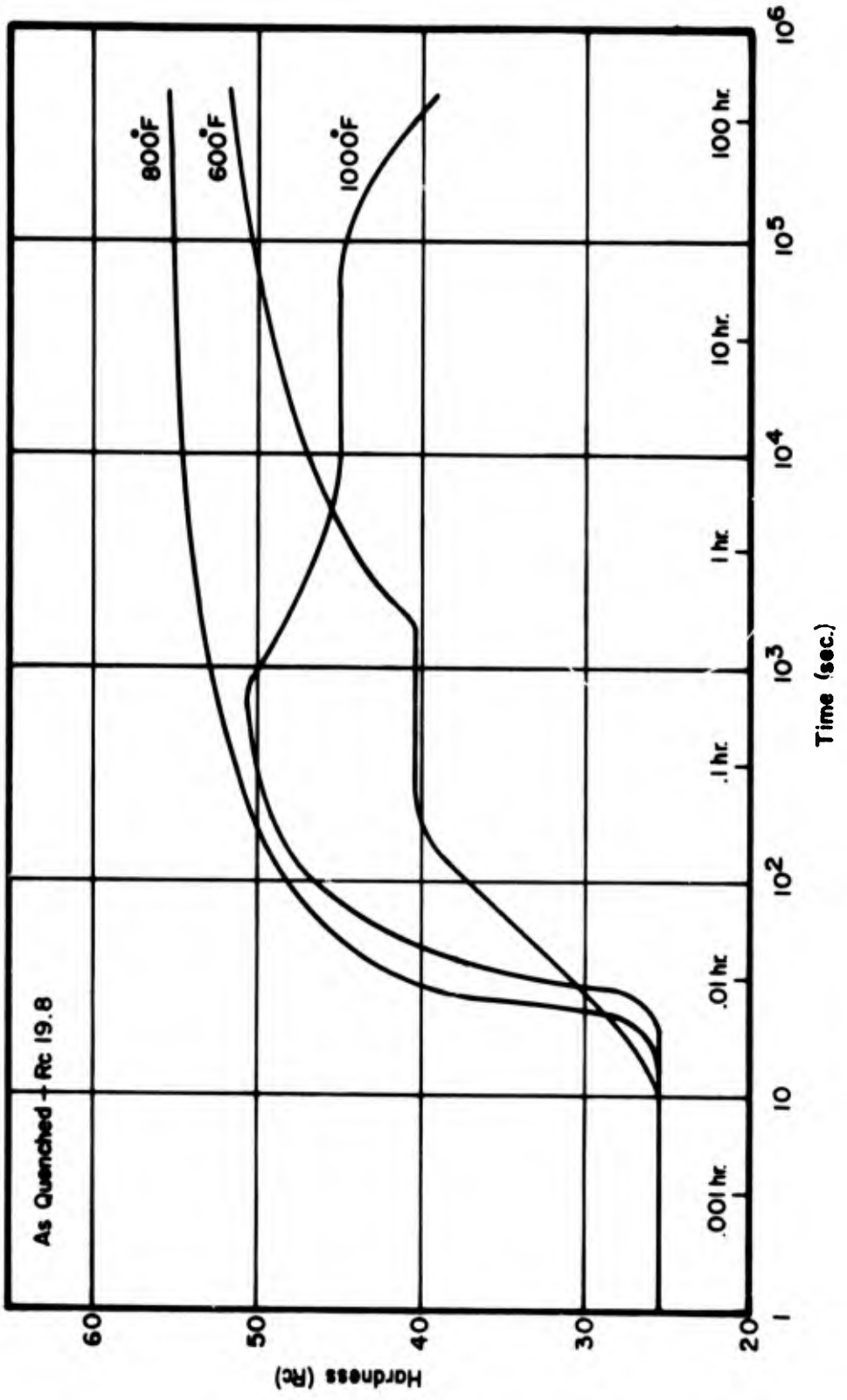

Figure 9. Aging transformation hardness - 905 alloy. Water quenched from 1650°F (900°C) prior to transformation.

A. 0.1 hour, 400X.

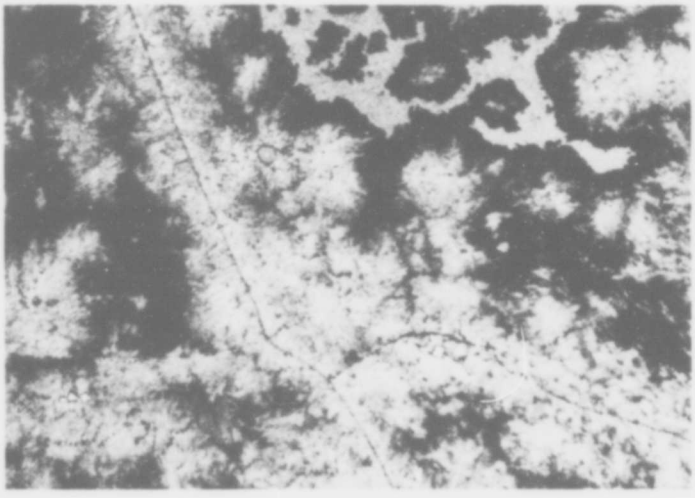

B. 10 hours, 400X.

Figure 10. Structure of the 905 alloy quenched and aged at 1000°F (538°C).

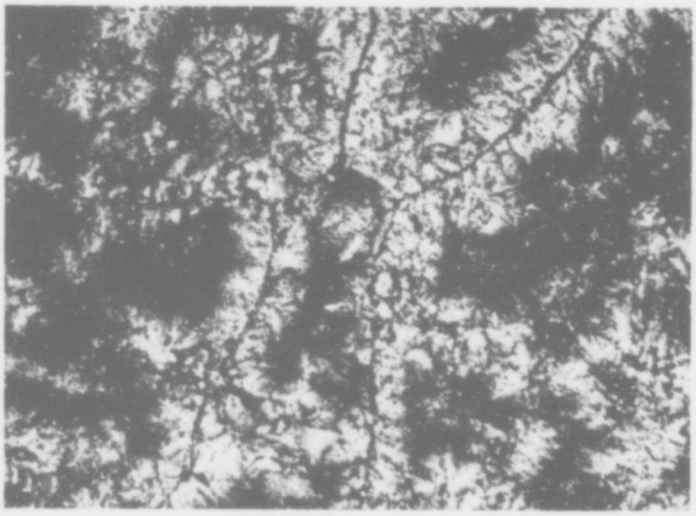

C. 46 hours, 400X.

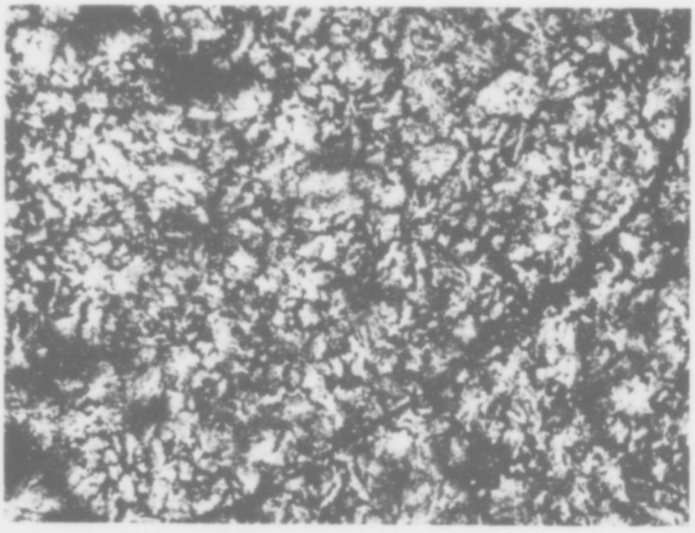

D. 46 hours, 800X.

Figure 10 (continued). Structure of the 905 alloy quenched and aged at 1000°F (538°C).

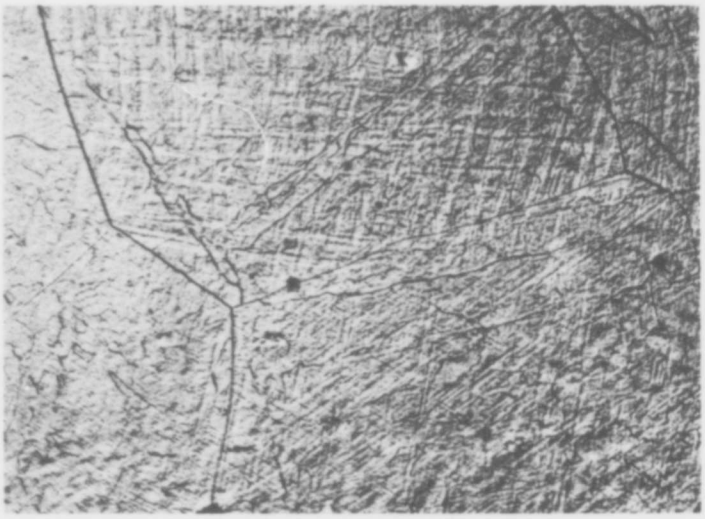

4 hours, 400X

Figure 11. Structure of the 905 alloy quenched and aged at 800°F (427°C).

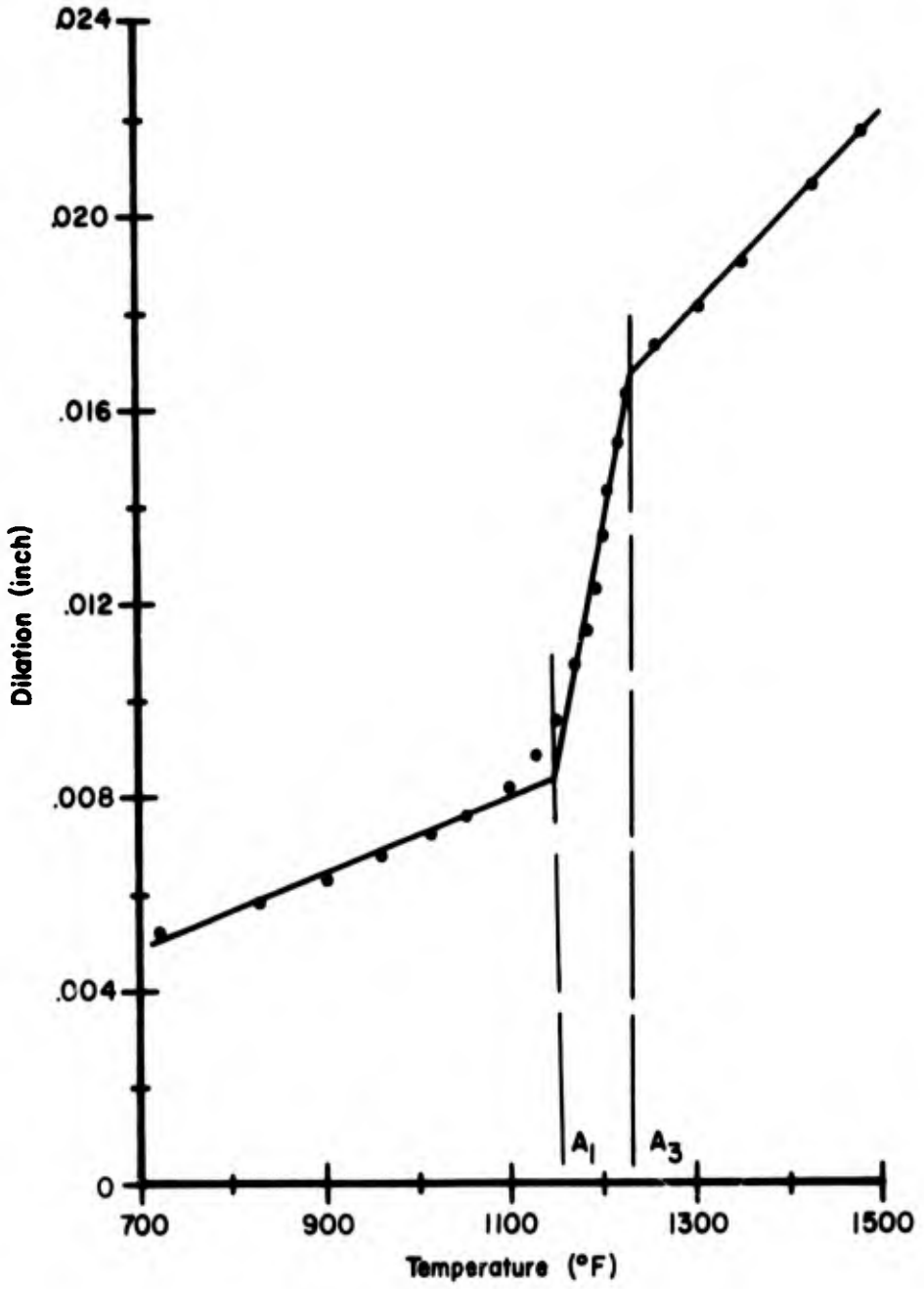

Figure 12. Dilation vs. temperature - 904 alloy. Slow heating.

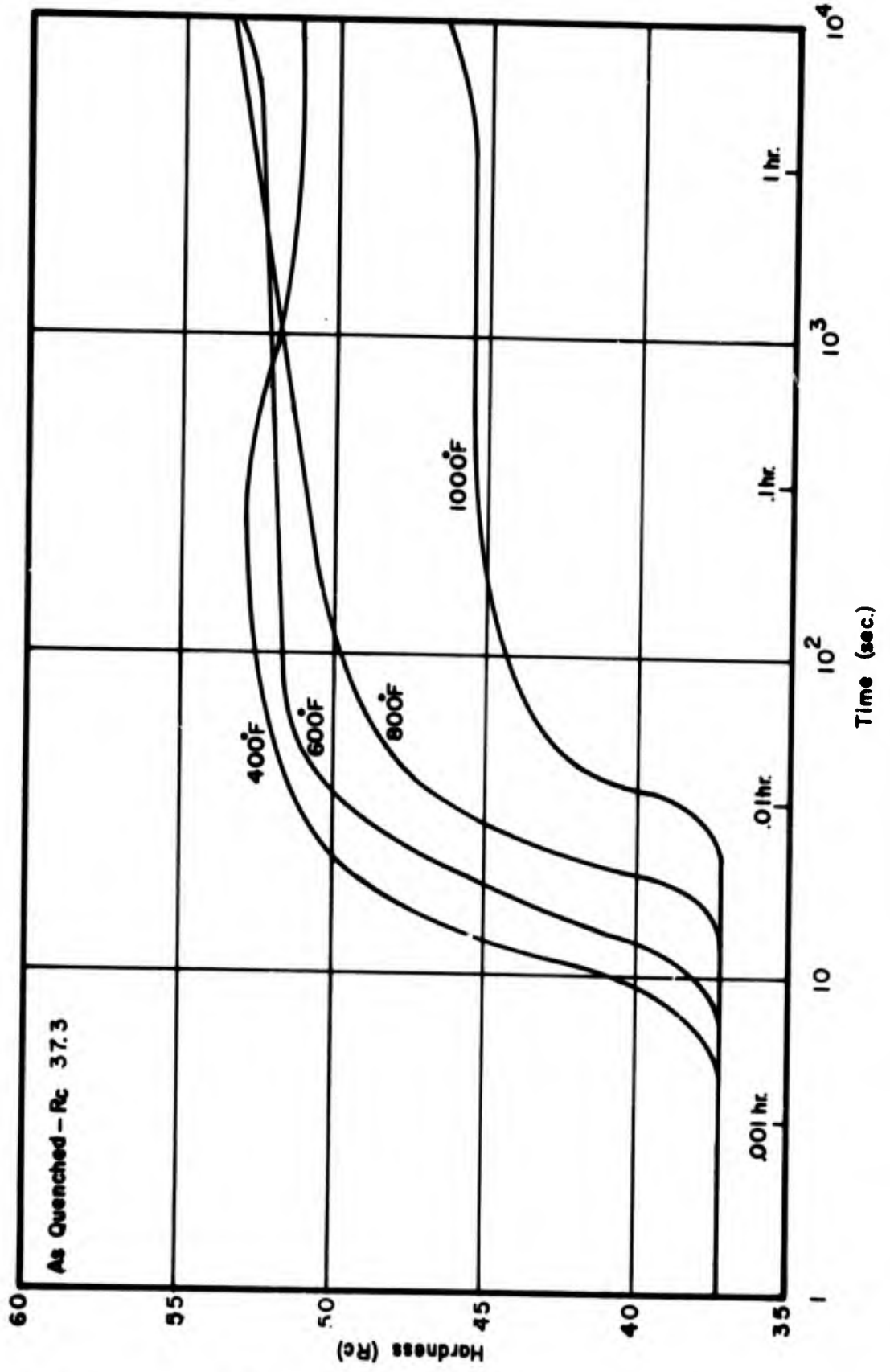

Figure 13. Isothermal transformation hardness - 904 alloy. Quenched to temperature from 1650°F (900°C).

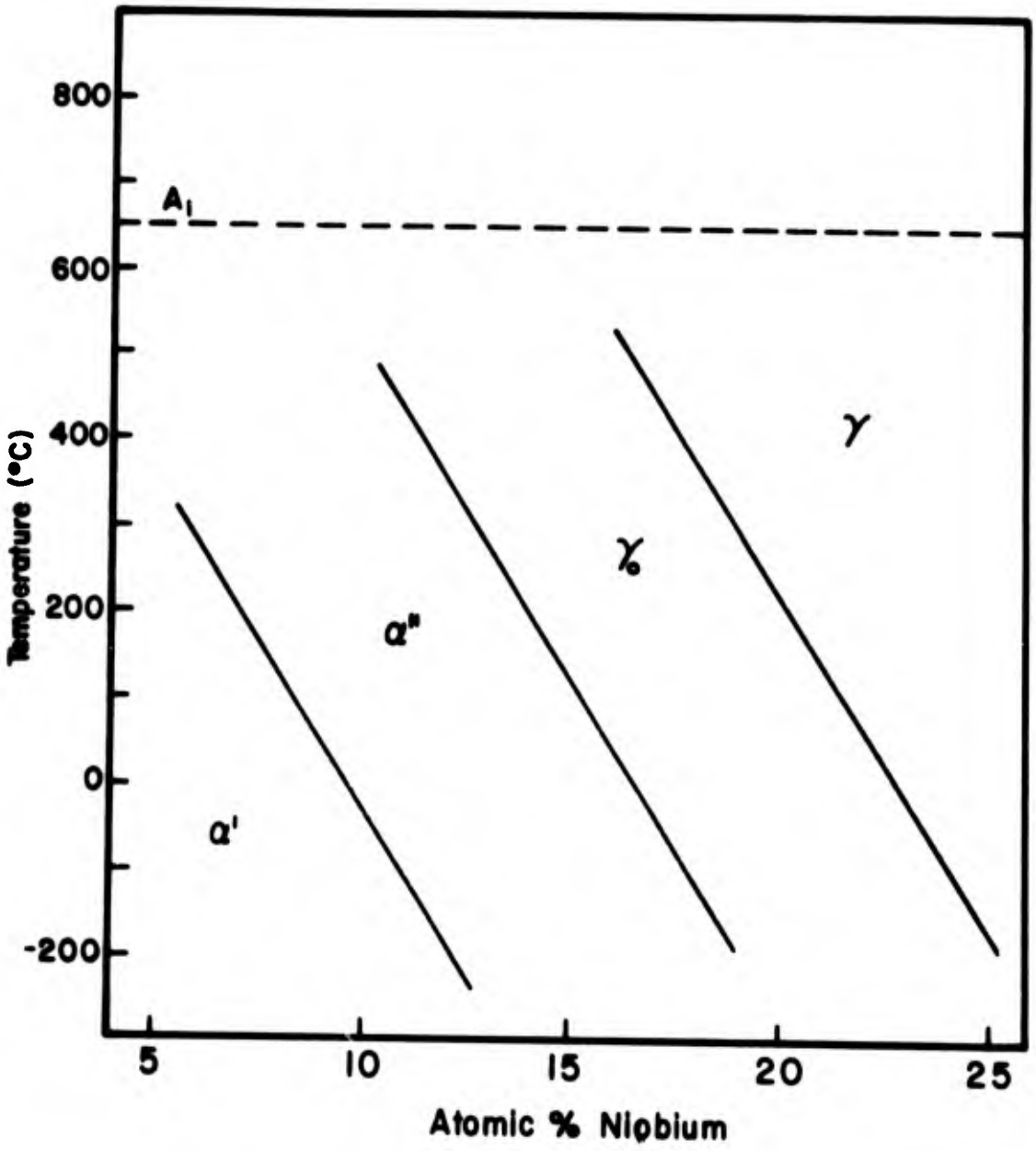

Figure 14. The effect of temperature and alloying content on uranium base alloys. (22).